



# Agricultural intensification vs climate change: What drives long-term changes of sediment load?

5 Shengping Wang<sup>1,2,3\*</sup>, Peter Strauss<sup>2</sup>, Carmen Krammer<sup>2</sup>, Elmar Schmalz<sup>2</sup>,  
Borbala Szeles<sup>3,4</sup>, Günter Blöschl<sup>3,4</sup>

1. *College of Hydraulic and Hydro-Power Engineering, North China Electric Power University, Beijing, 102206, P.R.China*

2. *Institute for Land and Water Management Research, Federal Agency for Water Management, A-3252 Petzenkirchen, Austria*

10 3. *Institute of Hydraulic Engineering and Water Resources Management, Vienna University of Technology, Vienna, Austria*

4. *Vienna Doctoral Programme on Water Resource Systems*

**\*Corresponding author:** Shengping Wang

Email: wangshp418@126.com; Shengping\_Wang@ncepu.edu.cn

15

**Abstract:** Climate change and agricultural intensification are expected to increase soil erosion and sediment production from arable land in many regions. However, so far, most studies have been based on short-term monitoring and/or modeling, making it difficult to assess their reliability in terms of long-term changes. We present the results from a unique data set consisting of measurements of sediment loads from a 60ha catchment (the HOAL Petzenkirchen in Austria) over a time window spanning 72 years. Specifically, we compare Period I (1946-1954) and Period II (2002-2017) by fitting sediment rating curves for the growth and dormant seasons for each of the periods. The results suggest a significant increase in sediment yield from Period I to Period II with an average of  $11.6 \pm 10.8$  ton $\cdot$ yr $^{-1}$  to  $63.6 \pm 84.0$  ton $\cdot$ yr $^{-1}$ . The sediment

20

25



flux changed mainly due to a shift of the sediment rating curves (SRC), given that the annual streamflow varied little between the periods ( $5.6 \text{ l s}^{-1}$  and  $7.6 \text{ l s}^{-1}$ , respectively, on average). The slopes of the log regression lines of the SRC for the growing season and the dormant season of Period I were 16.72 and 4.9, respectively, whilst they were 5.38 and 1.17 for Period II, respectively. Climate change, considered in terms of rainfall erosivity, was not responsible for this shift, given that erosivity decreased by 30.4% from the dormant season of Period I to that of Period II, and no significant difference was found between the growing seasons of Periods I and II. However, the sediment flux changes can be explained by changes in crop type and parcel structure. During low and median streamflow conditions (*i.e.*  $Q < Q_{20\%}$ ), land consolidation in Period II (*i.e.* the parcel effect) did not exert an apparent influence on sediment production. Whilst with increasing stream flow ( $Q > Q_{20\%}$ ), parcel structure played an increasingly role in sediment yield contribution, and leading to a dominant role due to enhanced sediment connectivity in the landscape at extremely high flow conditions (*i.e.*  $Q > Q_{2\%}$ ). The increase in cropland in Period II at the expense of grassland had an unfavourable effect on sediment flux, independent of streamflow, with declining relevance as flow increased. We conclude that both land cover change and land consolidation should be accounted for simultaneously when assessing sediment flux changes. Especially during extremely high flow conditions, land consolidation substantially alters sediment fluxes, which is most relevant for long-term sediment loads and land degradation. Increased attention to improving parcel structure is therefore needed in climate adaptation and agricultural catchment management.



50 **Keywords: Sediment regime; Land use/cover change; Parcel structure;**  
**Climate change; Agricultural catchment**

## Introduction

Soil erosion is a risk of worldwide importance because of its environmental and  
55 economic consequences (García-Ruiz, 2010; Prosdocimi et al., 2016). Climate change,  
land use/cover changes and other anthropogenic activities are commonly considered  
potential agents driving variation of soil erosion rates (Nearing et al., 2004;  
Jean-Baptiste et al., 2015; Zhang et al., 2021). The impacts of future climate  
projections or recently observed climate change on soil erosion have been explored in  
60 a number of studies (Nearing et al., 2004; Zhang and Nearing., 2005; Mullan, 2013;  
Jean-Baptiste et al., 2015; Palazon and Navas, 2016; Mullan et al., 2019). Changes in  
land use or land cover have also been widely investigated, using either experimental  
observations or modelling approaches at various scales (e.g. Korkanç et al., 2018;  
Silva et al., 2017; Bochet et al., 2006; Karvonen et al., 1999; Ozsahin et al., 2018;  
65 Nampak et al., 2018; Li et al., 2019; Perović et al., 2018). Additionally, the relative  
contributions of climate change and land use/cover change have been increasingly  
investigated in recent years as both agents usually exert their influence on soil erosion  
simultaneously. In a review on anthropogenic and climatic impacts on Holocene  
sediment dynamics of the Western Mediterranean basin (Bellin et al., 2013), the  
70 impacts of climatic and anthropogenic activities on sediment dynamic were found to



interact with each other during moist climatic periods, whilst the enhanced sediment load was found only closely associated with enhanced aridity during dry climatic periods, independent of the intensity and type of human activities. By using field investigation combined with modeling, Zhang et al. (2021) quantitatively evaluated the contribution of climate change, land use, and silt trap dams to sediment reduction of a typical Loess watershed over 1987-2016, with contribution values being 29%, 40%, and 31%, respectively. Sun et al. (2020) quantified the contribution of climate change and land-use change to sediment reduction of a Loess watershed over 1997 to 2016, in which both engineering measures and land-use change accounted for 62% and 23 - 42% of sediment reduction, respectively, the rest being explained by climate change. Management practices generated a higher impact on soil erosion at the plot scale than climate change (Scholz et al., 2008). Also, livestock grazing accelerated soil erosion more than climate change in Qinghai-Tibet Plateau (Li et al., 2019).

The previous findings provide valuable information for implementing water and soil conservation measures and improving agricultural productivities (Nampak et al., 2018; Li et al., 2019). However, the role of landscape structure changes has so far not received much attention, even though land-use policies such as land consolidation have been changing agricultural practices to a large extent since the beginning of agricultural industrialization after 1945 (e.g. Moravcová et al., 2017; Devaty et al., 2019) and in particular in countries where the industrialization of agriculture is relatively recent (Bouma et al., 1998; Moravcova et al., 2017; Zhang et al., 2021). Landscape structures usually influence erosion due to the boundary effects between



land uses and land units (parcels) that differ in water and sediment trapping capacity (Baudry and Merriam, 1988; Merriam, 1990; Takken et al., 1999; Phillips et al., 2011).

95 Van Oost et al. (2000) and Devaty et al. (2019) evaluated the role of landscape structure by accounting for its spatial connectivity using modelling approaches and found that landscape structure is an essential factor when assessing the risk of soil erosion affected by land-use changes. Both studies emphasized the potential impacts of parcel structure changes on sediment production through altering hydrological and

100 sediment connectivity. However, both authors relied on models, making connectivity assumptions in their studies. Instead of focusing on the spatial connectivity, others (e.g. Bakker et al., 2008; Sharma et al., 2011; Chevigny et al., 2014; Wang et al., 2021; Tang et al., 2021; Madarász et al., 2021) evaluated the effect of terrain, soil properties, lithology, management practices and other processes associated with landscape and/or

105 land structure changes and highlighted their impact on sediment production. It has also been shown that the impact of landscape structure on erosion is more heterogeneous when different crops are grown, and the underlying lithology, soil properties and topography show substantial spatial variability across the catchment (David et al., 2014; Cantreul et al., 2020).

110 Even though numerous studies have addressed the effect of climate change and land management on soil erosion and sediment production, most studies have been based on short-term monitoring and/or modeling, which makes it difficult to assess their reliability in terms of long-term changes that are the most relevant from a practical perspective. This paper aims at evaluating the relative roles of climate change, land



115 use and land cover changes (LUCC) and change of land structure on sediment  
production. We present the results from a unique data set consisting of measurements  
of sediment loads from a small agricultural catchment over a time window spanning  
72 years. The catchment is the 66 ha Hydrological Open Air Laboratory (HOAL)  
Petzenkirchen (Blöschl et al., 2016), which, in addition to being exposed to climate  
120 change, has experienced a significant change in land use and land cover as well as  
parcel structure for erosion control during the past decades. Both discharge and  
sediment yield have been monitored in the HOAL catchment since the 1940s. This  
provides an opportunity for disentangling the impact of parcel structure and land  
use/land cover change, and the impact of climate change based on long-term  
125 measurements. Specifically, we aim at i) exploring how the sediment regime has  
changed between the periods of 1946-1954 and 2002-2017; ii) analyzing whether  
climate change or land-use changes (or both) were responsible for any change in  
sediment regime; and iii) identifying the relevance of land structure change (i.e. land  
consolidation) on erosion control compared to that of a change in land use or cover.

## 130 **2. Methods**

### **2.1 Catchment characteristics**

The HOAL catchment is situated in Lower Austria's alpine forelands (48°9' N, 15°9' E)  
with elevations ranging from 268 m to 323 m a.s.l. and a size of 66 ha. The climate of  
the catchment belongs to the temperate, continental climate zone (Dfb) according to  
135 Köppen-Geiger (Kottek et al., 2006), with a mean annual precipitation of 746 mm  
(1946 - 2006), 62% of the rain falling between May and October. The mean daily air



temperature is 8.8°C (1946-2006), and the dominant land use is arable land, accounting for, on average, 82% of the catchment over the past few years. Typical crops include winter wheat, corn and barley. Deciduous trees grow along the creek  
140 (6%), 10% of the area is grassland, and 2% is paved. The subsurface of the catchment consists of tertiary marine sediments. Soils are classified into five types: calcic cambisols, vertic cambisols, gleyic cambisols, planosols and gleysols (IUSS Working Group WRB, 2015).

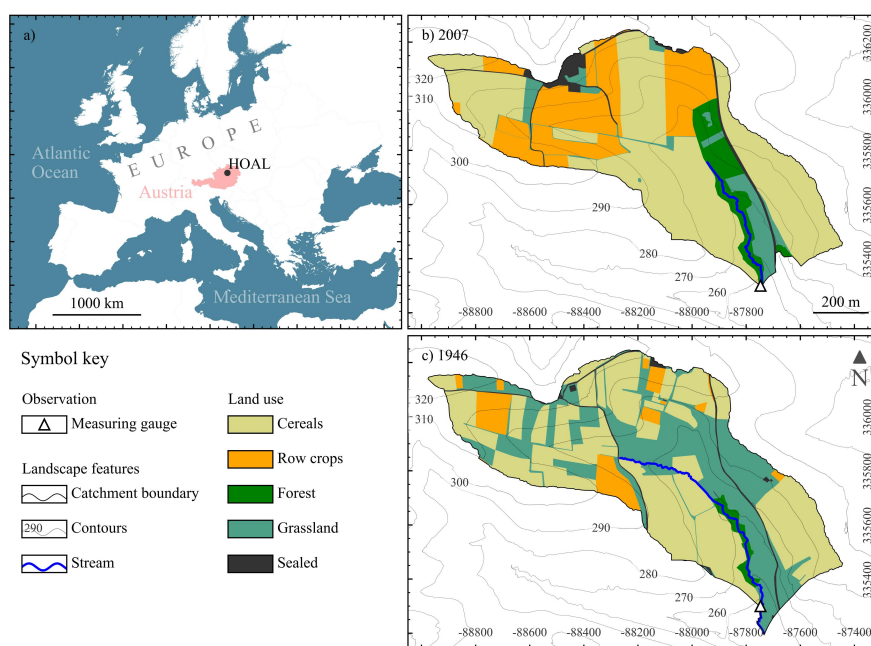
## 145 **2.2 Data availability**

Both streamflow discharge ( $Q$ , l/s) and sediment concentration ( $C$ , mg/l) have been measured at the catchment outlet since the 1940s. Data records from 1946-1954 (Period I) and 2002 to 2017 (Period II) were available for this analysis. Due to technological advances, the data was measured with different methods. In Period I,  
150 discharge was registered at 10 min resolution by a Thompson weir and a paper chart recorder, while in Period II, it was registered at 5 min resolution by an H-Flume and a pressure transducer. Sediment concentrations were measured manually every 3-4 days in Period I, whilst an automatic method plus additional manual sampling was applied in Period II. Daily precipitation and 5-min rainfall intensities were available for both  
155 periods, but for Period I, 5-min rainfall intensities were only available during the vegetation period.

We used parcel-based land use data from 1946 to 1949 and 2007 to 2012, representing Period I and Period II land use, respectively. Land use categories were agricultural land, including crop type, grassland, forest, roads and settlements. We defined a parcel



160 as a continuous area of land with a single crop type. Parcel boundaries were specified  
according to the cadastral map and aerial photographs. In Period II, these boundaries  
were also visually inspected. Figure 1 depicts the geographic catchment location, and  
parcel structure and land use for a specific year in each period.



165 Figure 1 Geographical location of the HOAL catchment in Petzenkirchen in Austria  
and Europe and Parcel structure and land use in the HOAL catchment for 1947 (a) and  
2007 (b). The black hatched area in b) represents a difference in catchment size due to  
the relocation of the stream gauge in Period II. Coordinates as EPSG: 31256 – MGI /  
170 Austria GK East (meters).

## 2.3 Data analysis

### 2.3.1 Changes in rainfall erosivity and flow regime

175 The effect of rainfall on erosion was quantified by the R-factor of the Revised  
Universal Soil Loss Equation (RUSLE), which is defined as the product of kinetic





energy of a rainfall event and its maximum 30-min intensity, using the rainfall erosivity tool RIST (USDA-Staff, 2019) according to

$$EI_{30} = \sum_{i=1}^m E_i \cdot I_{30,i} \quad (1)$$

180 where  $EI_{30}$  is the Annual R-factor ( $\text{N}\cdot\text{h}^{-1}\cdot\text{yr}^{-1}$ ) calculated as the sum of single event R-factors,  $E_i$  is the total kinetic energy for a single event ( $\text{kJ}\cdot\text{m}^{-2}$ ),  $I_{30}$  is the maximum rainfall intensity in 30 minutes within a single event  $i$  ( $\text{mm}\cdot\text{h}^{-1}$ ), and  $m$  is the number of events per year.

We assumed erosivity density  $ED$  (*i.e.*  $EI_{30}$  divided by event precipitation) to be a particularly relevant climatic indicator of the soil erosion process and catchment sediment yield. We, therefore, tested whether the means of the monthly erosivity density ( $ED$ ) are significantly different between Period I and Period II by using a t-test. Due to the absence of rainfall intensity measurements, we could not calculate  $ED$  for the months of the dormant season (November to March) of Period I. For this case, we calculated  $ED$  from a relationship between  $EI_{30}$  and monthly rainfall of 185 Period II, assuming that the relationship was sufficiently temporally invariant over the investigated periods. Erosivity is very low during the dormant season (Figure 3a); thus, the error arising from the use of this relationship is expected to be small.

We also compared daily flow duration curves to understand whether hydrological regime change has influenced flow transporting capacity and sediment regime 195 variation. Following the definitions of Smakhtin (2001), we compared low flow ( $Q_{70\%}$ ), high flow ( $Q_{10\%}$ ) and median flow rate ( $Q_{50\%}$ ) quantiles for the two periods.

### 2.3.2 Sediment regime analysis



Sediment regimes were mainly analyzed using sediment rating curves (SRC).

200 Following a common approach (Asselman, 2000; Warrick and Rubin, 2007; Sheridan  
et al., 2011; Vaughan et al., 2017; Khaledian et al., 2017), the SRCs were assumed to  
follow a power-law function, which was fitted by least squares regression:

$$C = a \cdot Q^b \quad (2)$$

where  $C$  is sediment concentration ( $mg\ l^{-1}$ ),  $Q$  is discharge ( $l\ s^{-1}$ ), and  $a$  and  $b$  are  
205 dimensionless regression coefficients. The coefficient  $a$  is usually associated with  
easily transported intensively weathered materials and may vary over seven orders of  
magnitude (Syvitski et al., 2000). The parameter  $b$  represents the capacity of the  
stream to erode and transport sediment, reflecting how sediment concentration is  
non-linearly related to streamflow (Sheridan et al., 2011; Fan et al., 2012). It typically  
210 varies from 0.5 to 1.5 and rarely exceeds 2. Sometimes  $b$  is also regarded as a measure  
of the quantity of new sediment sources available (Vanmaercke et al., 2010; Guzman  
et al., 2013).

Considering that data records were registered with different resolutions for Periods I  
and II (See section 2.2), for the sake of consistency, we used monthly averages, as  
215 conducted in the other studies (Syvitski and Alcott, 1995; Sheridan et al., 2011; Hu et  
al., 2011), to construct SRC. We assumed that monthly averages could reflect a varied  
hydrological and/or sediment response to seasonally prevailing weather characteristics  
such as dry periods or convective storms (Sheridan et al., 2011).

We chose arithmetic means of the observations to represent the monthly  $Q$  and  $C$   
220 values. These monthly averages were pooled together and then grouped into growing



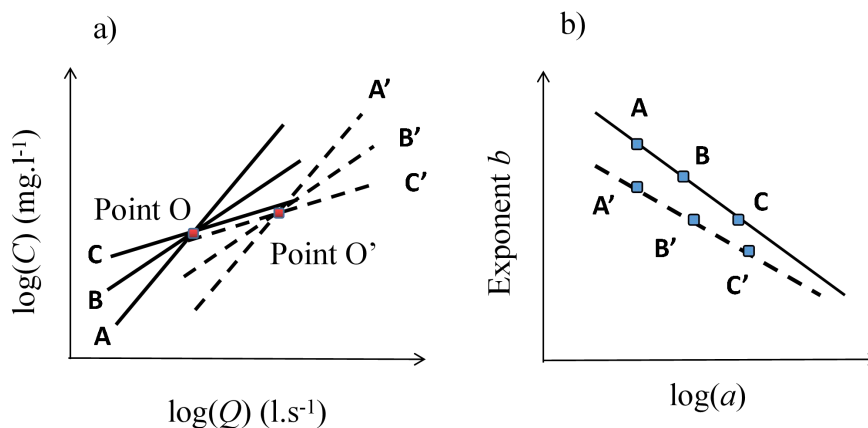
season of Period I (Period I\_G), dormant season of Period I (Period I\_D), growing  
season of Period II (Period II\_G), and dormant season of Period II (Period II\_D),  
respectively. For each of these four periods, we fitted SRC.

We analyzed the fitted SRC by two strategies to evaluate whether and how the  
225 sediment regime changed between these periods. Besides directly comparing the slope  
of the four seasonal SRC, we also fitted SRC by season and year and plotted the  
regression coefficients  $a$  against their corresponding  $b$  to evaluate a possible sediment  
regime shift during Periods I and II. Thomas (1988) suggested that this technique  
could exclude the interference of different sampling practices with the estimated  
230 sediment regime.

It is suggested that for the years (or catchments) with similar means of log-Q and  
log-C, SRC would usually pass through one common point O (Thomas, 1988;  
Syvitski et al., 2000; Desilets et al., 2007; Sheridan et al., 2011). This common point O  
(Figure 2a) is usually interpreted to reflect time invariant catchment characteristics,  
235 such as relief, drainage area, and drainage density, while the variation of the slope of  
SRCs (Figure 2a) is interpreted to reflect temporally dynamic characteristics, such as  
average or maximum discharge and sediment availability (Asselman, 2000). The  
coefficients  $a$  of the SRCs having a common point are usually inversely linearly  
related with  $b$  as well (Thomas, 1988, Syvitski et al., 2000 and Desilets et al., 2007).  
240 This provides a means for testing whether periods (or catchments) have similar  
sediment transporting regimes by plotting coefficient  $a$  against  $b$  (Figure 2b). That is  
to say, that the points plotted on the same line (A, B, C) in Figure 2b are representative



of periods (or catchments) having similar sediment transport regimes. Points A of  
 Figure 2b (upper-left-side) usually exhibit steeper rating curves than points C  
 (lower-right side). For different lines in Figure 2b, the lower ones represent situations  
 245 with most of the annual sediment load transported at relatively low flow discharge,  
 and the higher ones represent situations with suspended sediment mainly transported  
 at high streamflow. Thus, it is possible to reveal changes in sediment transport  
 regimes. Compared to a direct evaluation of rating curves, relating coefficient  $a$  to  
 250 exponent  $b$  is more conducive to revealing the temporal evolution of the sediment  
 regime (Syvitski et al., 2000; Desilets et al., 2007).



255 Figure 2 Schematic showing a) how sediment rating curves (SRC) may rotate  
 around a common point and b) how exponents  $b$  of the SRC relate to coefficients  $a$ . Lines A,  
 B and C on the left are SRC of different periods (e.g. years) sharing a similar common  
 point O. Once sediment regimes shift due to the changes in catchment characteristics  
 260 (change in drainage density, drainage area, and topography.....) the common point O  
 would change to point O', and the linear relationship between  $a$  and  $b$  of the SRC  
 would exhibit a shift as well. The schematic is based on  $\log C = \log a + b \log Q$   
 (Equation 2).



265 To account for uncertainties of the fitted SRC during each period, we additionally  
established theoretical sediment rating curves (tSRC); i) for each period (*i.e.* Period  
I\_G, Period I\_D, Period II\_G, and Period II\_D), we carried out random sampling of  
 $\log a$  ( $n=500$ , package "sample" in RStudio), assuming that the samples of the  
coefficient of  $\log a$  follow normal distributions (Figure 4), which was proved with a  
270 Kolmogorov-Smirnov test of normality (mean = 1.02, SD = 2.01,  $n=44$ ); ii)  
given the set of the sampled 500 values of  $\log a$ , we generated a set of  
values  $b$  according to the previously established linear relationship between  $\log a$  and  $b$ ;  
iii) given a set of specified Q values, we derived 500 tSRC for each period,  
corresponding to the paired  $\log a$  and  $b$  samples; iv) using these tSRC we calculated  
275 the 50 percentile, 5 percentile, and 95 percentile for each period to reveal uncertainties  
of the sediment rating curves.

The tSRC of the periods were also used to quantify the effect of land consolidation, *i.e.*  
change of parcels structure and sizes (Parcel\_effect) versus the effect of land use and  
land cover changes (LUCC\_effect). Since vegetation usually plays a minor role in the  
280 dormant season due to the absence of a dense vegetation cover on arable land and  
little erosive rainfall (Madsen et al., 2014; Kundzewicz, 2012; Salesa and Cerda, 2020;  
Hou et al., 2020), landscape structure in the dormant season was considered a  
critically important factor affecting runoff production and sediment production  
(Sharma et al., 2011; Devátý et al., 2019). Therefore, we hypothesized that the total  
285 change in sediment yield (Total effect) resulted from land cover change



(LUCC\_effect), land structure change (Parcel\_effect) and climate change (Climate\_effect). The effects of land cover and land structure change could be quantitatively separated according to the seasonal differences in tSRC after determining the climate change effect. Specifically, we assume that the shift of sediment regime from Period I\_D to Period II\_G is representative of the Total\_effect (Equation 3), and the shift in sediment regime between Period I\_D and Period II\_D is mainly due to land consolidation (Parcel\_effect) (Equation 4). Thus, the LUCC effect could be estimated according to Equation (5) if the Climate\_effect was insignificant (section 3.1). The contributions of Parcel\_effect and LUCC\_effect to the Total\_effect were estimated according to Equations (6) and (7), respectively.

$$\text{Total\_effect} = tSRC_{50\%}(\text{Period II\_G}) - tSRC_{50\%}(\text{Period I\_D}) \quad (3)$$

$$\text{Parcel\_effect} = tSRC_{50\%}(\text{Period II\_D}) - tSRC_{50\%}(\text{Period I\_D}) \quad (4)$$

$$\text{LUCC\_effect} = \text{Total\_effect} - \text{Parcel\_effect} - \text{Climate\_effect} \quad (5)$$

$$\text{Parcel\_effect (\%)} = \frac{\text{Parcel\_effect}}{\text{Total\_effect}} \times 100 \quad (6)$$

$$\text{LUCC\_effect (\%)} = \frac{\text{LUCC\_effect}}{\text{Total\_effect}} \times 100 \quad (7)$$

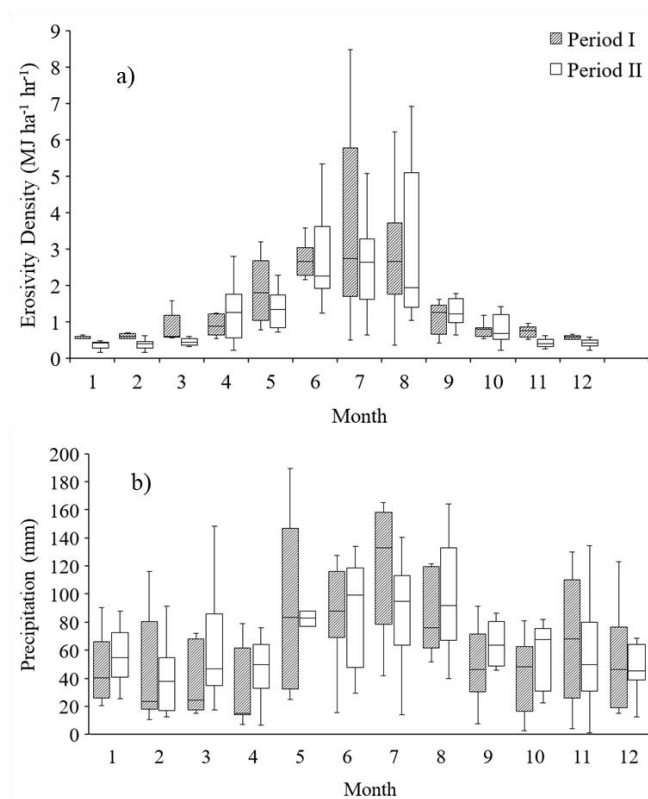
### 3. Results

#### 3.1 Changes in climate and flow regime

Because climate is commonly found responsible for hydrological change (e.g., Kelly et al., 2016; Wang et al., 2020), we compared erosivity density (*ED*) and monthly



precipitation ( $P$ ) of the two periods to examine whether climate affected the variation of sediment regime in the catchment. The mean monthly  $EDs$  in the growing season were  $2.37 \pm 1.38$  and  $1.84 \pm 0.86$  ( $N \cdot h^{-1} \cdot yr^{-1} \cdot mm^{-1}$ ) (standard deviation between years),  
310 respectively, which was not significantly different ( $p > 0.05$ ) between the first and second period (Figure 3a). In contrast, mean monthly  $ED$  in the dormant seasons showed a significant ( $p < 0.05$ ) decrease from the first to the second period ( $0.66 \pm 0.21$  and  $0.42 \pm 0.11$  ( $N \cdot h^{-1} \cdot yr^{-1} \cdot mm^{-1}$ ), respectively. No significant difference was found between the first and second periods for the mean monthly  $P$  in dormant or growing  
315 season (Figure 3b). The mean monthly  $P$  in Period I was  $50 \pm 33$  and  $76 \pm 54$  mm for the dormant and growing season, and  $53 \pm 29$  mm and  $79 \pm 47$  mm in Period II. The decrease in  $ED$  during the dormant season of Period II and the insignificant change in monthly  $P$  suggest that climate change between Period I and II was not responsible for an increased sediment availability (see section 3.3).



320

Figure 3 Distribution of a) monthly mean erosivity density and b) monthly precipitation for Periods I and II.

Daily flow duration curves for both periods are displayed in Figure 4. Generally, daily  
325 streamflow in Period I was higher than that of Period II. The  $Q_{70\%}$  low flow of the two  
periods was 2.3 and 1.9  $l.s^{-1}$ , the  $Q_{50\%}$  median flow was 3.1 and 2.7  $l.s^{-1}$ , and the  $Q_{10\%}$   
high flow was 7.3 and 6.5  $l.s^{-1}$ , respectively. The decreased flow regime of Period II,  
probably in part due to increased evapotranspiration over the past decades  
(Duethmann and Blöschl, 2018), suggests a smaller streamflow transport capacity and  
330 indicates that it was not responsible for the increased sediment transport in Period II  
(see section 3.3).



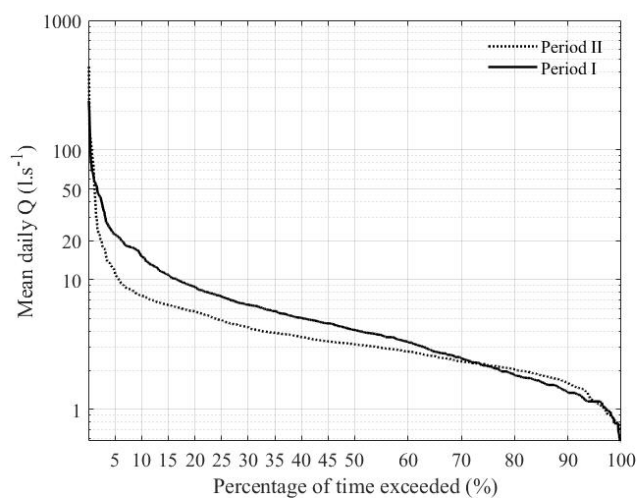


Figure 4 Mean daily flow duration curve for Periods I and II.

335

### 3.2 Change in land use and land organization

Table 1 shows how land use changed between the two periods. During Period I, cropland and grassland accounted for 73% to 82% and 14% to 22% of the area.

However, due to agricultural intensification, cropland increased to around 82% in

340 Period II, at the expense of a decreasing share of grassland. Forest, including sparse forest, accounted for 1.8% area during Period I but increased considerably until Period II to around 11%. Within the land use class of arable land, a substantial change from crops with low risk to cause soil erosion to crops with a high soil loss potential appeared. This was particularly true for maize. In addition, the diversity of crops  
345 decreased considerably (Table 2). This shift to agricultural uniformity is likely to affect also land structure effects.



Besides the change in land use, the parcel structure of the catchment also changed (Table 1). This change was related to a land consolidation plan issued in 1955 in Austria (Devátý et al., 2019) and a massive trend to agricultural industrialization that evolved after 1945. During Period I, arable land was fragmented across many small parcels, with a mean parcel size between 0.5 - 0.6 ha and a parcel density (number of parcels per ha area) between 1.7 - 2.0 ha<sup>-1</sup> in different years. In Period II, these values increased considerably to mean parcel sizes between 1.7 - 2.7 ha and parcel densities between 0.3 - 0.6 ha<sup>-1</sup>. Similarly, the mean parcel size and parcel density of grassland during Period I were 0.13 - 0.17 ha and 5.2 - 7.2 ha<sup>-1</sup>. It had changed to 1.06 ha and 0.9 ha<sup>-1</sup> in Period II.

**Table 1 Parcel and land use statistics for Periods I and II. Land use for the years 1946 to 1949 represents Period I, land use for the years 2007 to 2012 represents Period II; N is the number of parcels for a given land use, density is the number of parcels per ha, mean size represents the mean area of parcels with a particular land use.**

Land use	Parcel Structure							
	Period I				Period II			
	N	Density (1-ha <sup>-1</sup> )	Mean size (ha)	Area (%)	N	Density (1-ha <sup>-1</sup> )	Mean size (ha)	Area (%)
Arable land	70-111*	1.7-2.0	0.5-0.6	73-82	21-33	0.3-0.6	1.7-2.7	81-82
Grassland	70-81	5.2-7.2	0.1-0.2	14-22	6	0.9	1.1	3-4
Forest	1	-	1.2	1.8	7	1	1.0	10.5-11
Paved area	17	12.9	0.1	2	17	7.3	0.1	2.4

\* The number of parcels varied with the specific year of a period

365

**Table 2 Crop statistics of arable land for Periods I and II; Crop statistics for the years 1946 to 1949 represent Period I, crop statistics for the years 2007 to 2012 represent Period II; Erosion risk for a particular crop is classified as high or low according to the classification of management in the RUSLE.**

370

Period I	Period II
----------	-----------



	Area (ha)	Area (%)	Area (ha)	Area (%)	Erosion risk
Meadow	9-15	18-30	0.8	2	low
Alfalfa	11-18	22-33	-	-	low
Wheat	5-14	9-26	3-35	5-66	low
Rye	3-13	5-24			low
Beets	2-12	3-22	-	-	high
Oats	2-10	4-18	2	4	low
Barley	0.3-8	5-15	2-29	5-55	low
Potatoes	3-7	6-14	-	-	high
Maize	0.3-0.8	0.6-1.1	6.3-34	12-63	high
Rape	-	-	0.7-23	1-43	low
Sunflower	-	-	0.2-2	0.3-4	high

### 3.3 Change in sediment transport regime

#### 3.3.1 Direct comparison of the fitted SRCs

Figure 5 shows the fitted sediment rating curves ( $p < 0.05$ ) for both periods. Although  
 375 rainfall erosivity of Period II\_G was similar to that of Period I\_G (Figure 3a) and  
 streamflow of Period II was generally lower than that of Period I (Figure 4), the fitted  
 SRC of Period II\_G was steeper than that of Period I\_G (Figure 5a), with the  
 coefficients  $b$  being 0.32 and 1.65 for Period I\_G and Period II\_G, respectively (Table  
 3). The rating curves of the dormant seasons demonstrated a faster response of  
 380 sediment concentration to increasing flow in Period II\_D (Figure 5b), the coefficients  
 $b$  being 0.75 and 1.69 for Period I\_D and Period II\_D, respectively. However, the  
 rainfall  $ED$  in Period II\_D was generally lower than that of Period I\_D (Figure 3a),  
 suggesting a lower probability of a substantial increase in sediment availability. These  
 results indicate that neither changes in rainfall erosivity nor the hydrological regime  
 385 could explain the increase in sediment dynamics.

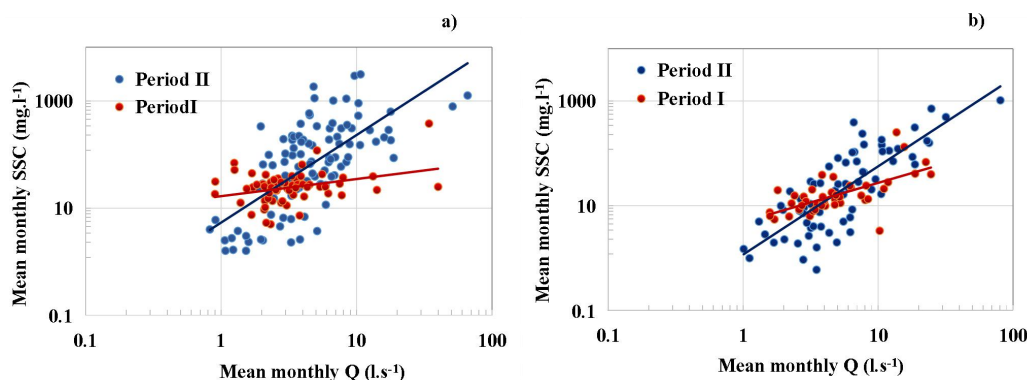


Figure 5 Sediment rating curves for a) the growing seasons and b) the dormant seasons in the two periods. Each point represents one mean monthly observation.

390

**Table 3** Parameter values for the coefficients of the SRC for different periods and seasons according to Equation (2).

Period	Coefficient		$r^2$
	$a$	$b$	
Period I_G	16.72	0.32	0.11
Period I_D	4.90	0.75	0.42
Period II_G	5.38	1.63	0.45
Period II_D	1.17	1.69	0.64

### 395 3.3.2 Relationship between coefficient $a$ and $b$

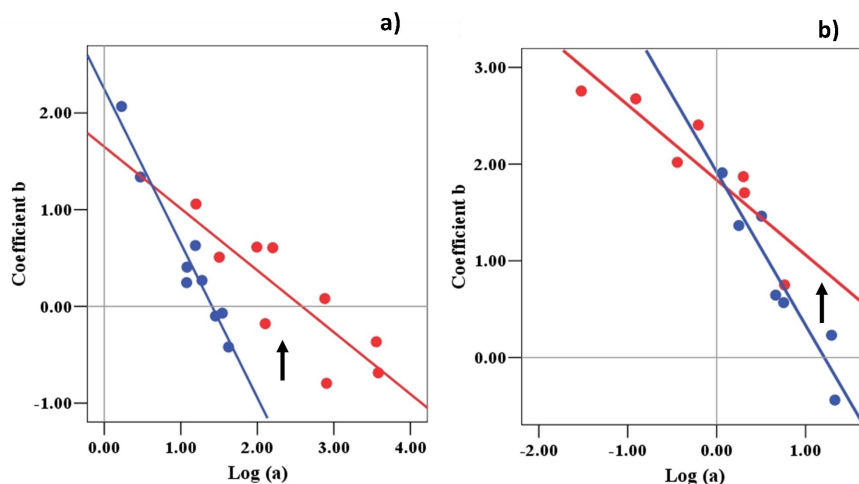
The changing steepness of a fitted SRC does not necessarily imply a change in sediment regime as slopes of fitted SRC sometimes are affected by catchment size or the distribution of samples (Asselman, 2000). To minimize possible interference of other factors in identifying variation or shift of SRC, we investigated the relationship

400 between coefficients  $a$  and  $b$  of the SRC. This technique was used by Asselman et al. (2000) and Fan et al. (2012) to examine the differences in sediment regimes between



spatially different sites. Additionally, Sheridan et al. (2011) used the relationship to reveal post-fire temporal shifts of a sediment regime.

Figure 6 displays the coefficients  $\log(a)$  plotted against  $b$  for the four investigated  
405 time frames. Even though monthly averages were used for the sake of consistency, the different sampling strategies of Periods I and II caused a biased distribution of  $\log(a)$  and  $b$ . Data of Period I is concentrated in the right-lower area (blue points). In contrast, data of Period II is more concentrated in the left-upper area, which is especially true during the dormant season.



410 Figure 6 Relationship between coefficients  $a$  and  $b$  for a) growing season and b) dormant season of Period I (blue) and Period II (red), respectively. All regressions are significant at  $p < 0.05$ .

415 Nevertheless, it is evident that the regression line exhibits a shift between the periods, the slopes of the regression line changing from -1.60 to -0.94 in the growing season and from -1.58 to -0.80 in the dormant season (Figure 6). The shift of the line to the



upper direction at log (a) larger than around 0.6 suggests that in Period II, most of the sediment was transported at relatively high flow rates. Since climate change was not responsible for the increased hydrological regime (see section 3.1), we mainly attribute this shift to the increase in hydrological connectivity, such as flow path density and flow length, and a change in land use and land cover statistics.

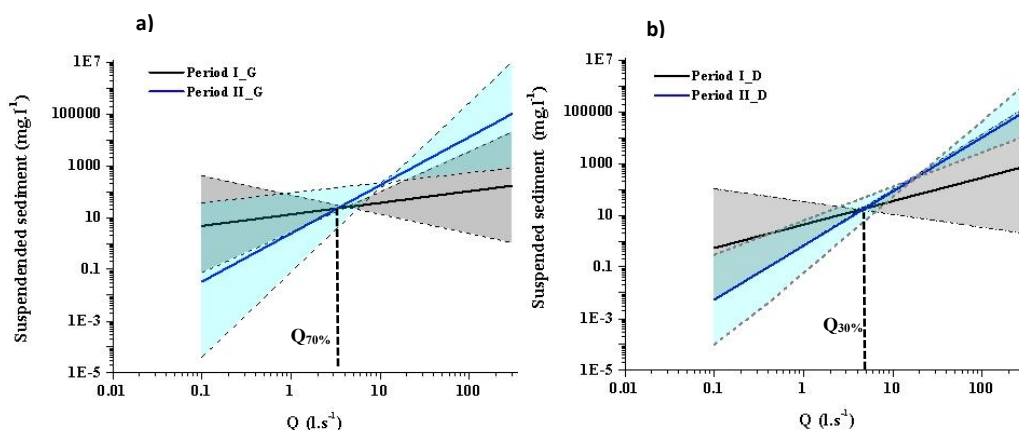


Figure 7 tSRC for the growing seasons (a) and the dormant seasons (b) of Period I and II. Solid lines denote the 50 percentile of the tSRC for each period. The grey area denotes the range of the predicted tSRC composed of 5 and 95 percentiles.  $Q_{30\%}$  and  $Q_{70\%}$  and represent the flow conditions of  $3.9 \text{ l.s}^{-1}$  and  $2.0 \text{ l.s}^{-1}$ , respectively.

Figure 7 displays the tSRC with their uncertainties for the different periods and seasons, to allow for directly discriminating the change in sediment regime with uncertainty. During most of the time, *i.e.* at flow rates larger than approximately  $Q_{70\%}$ , sediment concentrations for a given  $Q$  in Period II\_G were considerably higher than in Period I\_G (Figure 7a), whilst at flow rates below this value, sediment concentrations were not different. This finding is supported by the significant change in the sediment



load of  $6.3 \pm 19.9$  ton per month during Period II\_G compared to  $0.8 \pm 3.3$  ton per month during Period I\_G. Sediment concentration in the dormant season of Period II was considerably higher than that of Period I at flow rate exceeding  $Q_{30\%}$  (Figure 7b). Again, this confirms the shift of sediment transport regime in Period II\_D and is in  
440 line with the increase in sediment load in Period II\_D, resulting in mean monthly sediment loads of  $5.4 \pm 18.3$  ton per month compared to  $1.3 \pm 3.9$  ton for Period I\_D.

### 3.4 Parcel\_effect versus LUCC\_effect

Figure 8 demonstrates the dynamic contributions of land structure and land cover  
445 changes on sediment concentrations with increasing flow. Land consolidation and the substantial increase in cropland at the expense of a decrease in grassland explained the increase in sediment yield. However, the trends of their contributions to this increase differed. Generally, with higher flow rates, the contribution of the LUCC\_effect gradually decreased, whilst the contribution of the Parcel\_effect increased. The  
450 Parcel\_effect accounted for more than 50% of the Total\_effect after the flow rate exceeded  $20 \text{ l s}^{-1}$  approximately (*i.e.*  $Q_{2\%}$ ) (Figure 8), exhibiting a dominant role in sediment production. The opposite trend of the contributions between LUCC\_effect and Parcel\_effect suggests that, even though land consolidation and an increase in cropland both have unbeneficial effects on erosion control, their hydrological  
455 consequences may be different, with land structure change probably explaining much of the variation of sediment load at high flow conditions.

Unlike the situation during high flow rates, the Total\_effect showed an almost zero

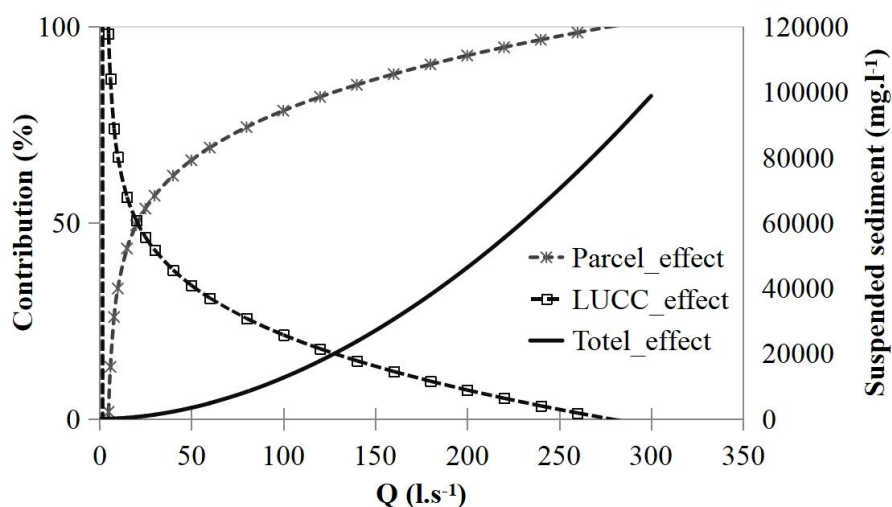


value at flow rates less than approximately  $2 \text{ l}\cdot\text{s}^{-1}$  (*i.e.*  $Q_{70\%}$ ) (Figure 8), suggesting no difference in sediment load between Periods I and II at low flow conditions. The

460 increase in sediment load, at flow rates of 2 up to around  $20 \text{ l}\cdot\text{s}^{-1}$ , seemed mainly due to the increase in the cropland of Period II, as the contribution from LUCC\_effect was consistently higher than that of the Parcel\_effect.

One may note that forest cover increased considerably from Period I to Period II. It, however, did not show an influential role in erosion control. We hypothesize that even

465 though a beneficial effect of forest increase (accounting for 11% around of the catchment) may have appeared in Period II, it was offset by the negative effect of crop land changes, particularly the increase in erosive row crops, which contribute substantially to sediment yield compared with other land uses and other crop types (Kijowska - Strugała et al., 2018).



470 Figure 8 Contribution of Parcel\_effect and LUCC\_effect to the Total\_effect across various flow rates. Total\_effect (Equation 3) is displayed in terms of suspended sediment concentration. Parcel\_effect and LUCC\_effect was estimated by Equations





(4) and (5), respectively; their contribution to the Total\_effect was estimated by  
475 Equations (6) and (7), respectively.

#### 4. Discussion

Industrial intensification of agriculture implemented in the last 70 years has raised  
480 considerable concern regarding erosion and sediment loading of rivers (e.g. Bakker et  
al., 2008; Chevigny et al., 2014). However, with global climate warming, the different  
contributions to sediment load from land use and land cover change, land policy  
adjustments such as land consolidation and climate change are not well understood.  
This paper aims at evaluating the relative roles of climate change, land use and land  
485 cover changes, and land consolidation in sediment production, particularly for varying  
flow rates.

We found that sediment load increased substantially from Period II to Period I.  
Climate change in terms of both monthly  $ED$  and  $P$  was not responsible for this effect,  
instead it can be explained by land cover and land consolidation changes. Their  
490 relative contributions varied with streamflow. For flow conditions below around 5  
 $l.s^{-1}$  (i.e.  $Q_{20\%}$ ), land consolidation had no apparent adverse effect on erosion control,  
but with increasing flow, the contribution to sediment load increased continuously,  
leading to a dominant role at extremely high flow rates. This finding is partially in  
line with David et al. (2014) and Cantreul et al. (2020). They reported that landscape  
495 structure was less important for soil erosion during most normal flow conditions than  
land use and land cover. However, they did not investigate whether the effect of  
landscape structure showed a dynamic behavior with increasing flow. In contrast, the



LUCC\_effect, i.e. the increase of crops with high erosion risk, continuously affected sediment load with gradually decreasing importance for high and extreme flow conditions. Similar results have been reported by Vaughan et al. (2017), who showed that sediment concentration at low and median flow conditions was considerably associated with a change in catchment characteristics, primarily land use and land cover.

Although the effect of land use changes was dominating for flow conditions below  $Q_{20\%}$ , its contribution to the total annual sediment load was small. More than 75% of the total sediment load was transported during a small number of events (25 events in Period I, 8 events in Period II) and all events had flow rates above  $15 \text{ l.s}^{-1}$ , which underlines the importance of land structure for sediment loading.

This behavior is associated with the processes and mechanisms of vegetation controlling overland flow as a transporting agent for sediment (e.g. Sun et al., 2013; El Kateb et al., 2013; Nearing et al., 2017; Kijowska - Strugała et al., 2018; Silasari et al., 2017). A change in land use and land cover implies alterations of surface characteristics, such as above ground structure morphology, litter cover, organic matter components, root network (Gyssels et al., 2005; Wei et al., 2007; Moghadam et al., 2015; Patin et al., 2018) and soil properties (Costa et al., 2003; Moghadam et al., 2015). These properties influence the protective role of vegetation in soil detachment, flow capacity to transport sediment particles, and runoff flow paths to river channels (Van Rompaey et al., 2002; Lana-Renault et al., 2011; Sun et al., 2018). Nevertheless,



520 the protective effects do not linearly increase with increasing surface runoff.

Accelerated discharge and stronger scouring effects of upslope discharge might impair the protective role of vegetation (*e.g.* Zhang et al., 2011; Santos et al., 2017; Yao et al., 2018; Bagagiolo et al., 2018; Wang et al., 2019). Vegetation usually exhibits a smaller interception capacity at high rainfall intensity, resulting in enhanced splash erosion

525 and availability of mobile soil particles (Cayuela et al., 2018; Magliano. et al., 2019; Nytych et al., 2019). However, the decreasing contribution of the LUCC\_effect does not directly imply an absolute decrease of the magnitude of the LUCC\_effect. The absolute change in SSC resulting from LUCC reveals an increasing trend as flow rates increases. Thus, the contribution of the LUCC\_effect stands for the relevance of

530 LUCC in erosion control compared to the change due to land consolidation. The magnitude of the LUCC\_effect probably depends mainly on where within the catchment the land cover was replaced and how the proportional area of various land uses changed. We will address this issue in future analyses.

Unlike land cover and land use change, landscape structure is usually combined with

535 other catchment properties, such as slope characteristics and soil properties (Gascuel-Oudoux et al., 2011) and additional erosion and transport factors (Verstraeten et al., 2000), exerting a more complicated influence on erosion control. For example, the effect of landscape structure on soil erosion may be identified on moderate slopes, while on steep slopes it may be concealed by on-site severe soil erosion (Chevigny et

540 al., 2014). However, the key process for erosion control is the fact that landscape elements and their structural position (*i.e.* parcel structure, field boundaries, hedges



and similar) alter hydrological connectivity between land and water. This is particularly true when the land cover on both sides of boundaries is different (Van Oost et al., 2000). Reducing parcel size and heterogeneity increases hydrological connectivity significantly and results in a substantial off-site damage effect, irrespective of on-site erosion of the investigated land use (Boardman et al., 2018; Devátý et al., 2019). During low and median flow conditions, surface runoff and sediment may arrive to a lesser extent at field boundaries due to efficient interception effects of the vegetation cover. This may explain the identified dynamic relevance of land structure change in sediment load herein.

Our findings are also supported by the calculation of the management factor (C-Factor) and the slope and slope length factor (SL-Factor) of the RUSLE for Period I and Period II. While the mean C-Factor of the HOAL catchment increased from 0.16 during Period I to 0.33 for Period II, the SL factor increased from 0.76 to 0.96 from Period I to Period I. Taken together, the changed values for these two factors increase the theoretical soil loss within the catchment by over 150%. This is smaller than the changes observed, however it should be noted that the RUSLE has not been designed to account for sediment loads of catchments but to estimate field scale soil loss within catchments. This may explain the observed differences to a certain extent.

560

## 5 Conclusions

Climate change, land use and cover change, and other human-associated activities are widely regarded as potential agents driving hydrological change. Understanding the



relevance of each of these factors in the hydrological cycle is critical for

565 implementing adaptive catchment management measures and addressing climate  
change. For some hydrological cycle components, very significant climate change  
influences in the last decades have been identified (e.g. Haslinger et al., 2019;  
Duethmann and Blöschl, 2018). However, we found that climate change in rainfall  
erosivity and precipitation cannot explain the increased sediment production between

570 1946-1954 and 2002-2017 in the investigated catchment. Instead, both land cover and  
land consolidation played dynamic roles in controlling erosion.

Still, the relevance of land use and land cover change versus land consolidation  
change varied dynamically with changing flow conditions. The reduction in parcel  
density undoubtedly increases soil erosion risk, particularly at higher flows due to the

575 decreased capacity of trapping sediment particles between parcels and increasing flow  
lengths inside parcels. Meanwhile, unfavorable land use or land cover change will  
increase sediment load at most normal flow conditions, although the relevance of this  
process would decrease at high or very high flow rates. Therefore, when addressing  
soil conservation measures at the catchment scale, the distribution of fields, land

580 structure, and vegetation cover should be simultaneously considered. Such a strategy  
would be conducive to dealing with the risk of soil erosions at different flow rates.  
Land use policy adjustments resulting from technological development have been  
vital to deal with food security issues in the past. However, now we have to  
experience the negative influence of these adjustments on the hydrological cycle.

585 Therefore, rather than focusing on climate change solely, we need to pay increased



attention to anthropic management activities to counteract their negative impact on hydrological change effectively.

### **Author contributions**

590 Shengping Wang has led the data analysis, drafted the manuscript, and revised the manuscript; Peter Strauss was responsible for the project design, oversaw the whole analysis, and conduct manuscript revision as the project leader; Carmen Krammer was responsible for data collection and data preparation; Elmar Schmaltz has contributed to figure drawing and manuscript revision; Borbala Szeles has helped to revise the  
595 manuscript, and Günter Blöschl oversaw and critically reflected on the manuscript revision as the senior scientist.

### **Competing interests**

The authors declare that they have no conflict of interest.

600

### **Disclaimer**

Publisher's note: Copernicus Publications remains neutral with regard to jurisdictional claims in published maps and institutional affiliations.

605

### **Acknowledgements**

This work is financially supported by the SHUI project (Soil Hydrology research platform underpinning innovation to manage water scarcity in European and Chinese cropping systems) within the Horizon 2020 Research and Innovation Action of the  
610 European Community (No. 773903), the Austrian Science Funds (FWF), project W1219-N28, and the TU Wien Risk network.



## References

- Asselman, N. E. M. 2000. Fitting and interpretation of sediment rating curves. *Journal of Hydrology*, 234(3-4), 228-248. [https://doi.org/10.1016/S0022-1694\(00\)00253-5](https://doi.org/10.1016/S0022-1694(00)00253-5).  
615
- Bagagiolo, G., Biddoccu, M., Rabino, D., Cavallo, E. 2018. Effects of rows arrangement, soil management, and rainfall characteristics on water and soil losses in Italian sloping vineyards. *Environmental Research* 166: 690-704.
- Bakker, M., Govers, G., van Doorn, A., Quetier, F., Chouvardas, D., Rounsevell, M. 2008. The response of soil erosion and sediment export to land-use change in four areas of Europe: The importance of landscape pattern. *Geomorphology* 98:213-226.  
620
- Baudry, J. and Merriam, H.G. 1988. Connectivity in landscape ecology. Proc. 2nd Intern. Semin. of IALE, Muenster 1987. *Muensterische Geographische Arbeiten* 29: 23-28.
- Bellin, N., Vanacker, V., De Baets, S. 2013. Anthropogenic and climatic impact on Holocene sediment dynamics in SE Spain: A review. *Quaternary International* 308-309 :112-129.  
625
- Bochet, E., Poesen, J., Rubio, J.L. 2006. Runoff and soil loss under individual plants of a semi-arid Mediterranean shrubland: influence of plant morphology and rainfall intensity. *Earth Surf. Process. Landforms*. 31, 536-549.
- Bouma, J., Varallyay, G., Batjes, N.H. 1998. Principal land use changes anticipated in Europe. *Agr. Ecosyst. Environ.* 67 (2-3): 103-119.  
630
- Blöschl, G., Blaschke, A. P., Broer, M., Bucher, C., Carr, G., Chen, X., Eder, A., Exner-Kittridge, M., Farnleitner, A., Flores-Orozco, A., Haas, P., Hogan, P., Kazemi Amiri, A., Oismüller, M., Parajka, J., Silasari, R., Stadler, P., Strauss, P., Vreugdenhil, M., Wagner, W., and Zessner, M. 2016. The Hydrological Open Air Laboratory (HOAL) in Petzenkirchen: a hypothesis-driven observatory, *Hydrol. Earth Syst. Sci.*, 20, 227-255, doi:10.5194/hess-20-227-2016.  
635
- Cantreul, V., Pineux, N., Swerts, G., Biélders, C., Degré, A. 2020. Performance of the LandSoil expert-based model to map erosion and sedimentation: application to a cultivated catchment in central Belgium. *Earth Surf. Process. Landforms*. DOI: 10.1002/esp.4808.
- Cayuela, C., Llorens, P., Sanchez-Costa, E., Levia, D.F., Latron, J. 2018. Effect of biotic and abiotic factors on inter- and intra-event variability in stemflow rates in oak and pine stands in a Mediterranean mountain area. *Journal of Hydrology*, 560: 396-406.  
640
- Chevigny, E., Quiquerez, A., Petit, C., Curmi, P. 2014. Lithology, landscape structure and



- management practice changes: Key factors patterning vineyard soil erosion at metre-scale spatial resolution. *CATENA* 121:354-364.
- 645 Costa, M.H., Botta, A., Cardille, J.A., 2003. Effects of large scale changes in land cover on the discharge of the Tocantins River, Southeastern Amazonia. *J. Hydrol.* 283, 206-217.
- David, M., Follain, S., Ciampalini, R., Le Bissonnais, Y., Couturier, A., Walter, C. 2014. Simulation of medium-term soil redistributions for different land use and landscape design scenarios within a vineyard landscape in Mediterranean France. *Geomorphology* 214: 10-21
- 650 Desilets, S.L.E., Nijssen, B., Ekwurzel, B., Ferre, T.P.A., 2007. Post-wildfire changes in suspended sediment rating curves: Sabino Canyon, Arizona. *Hydrol. Process.* 21,1413-1423.
- Devátý, J., Dostál, T., Hösl, R., Krása, J., Strauss, P. 2019. Effects of historical land use and land pattern changes on soil erosion - Case studies from Lower Austria and Central Bohemia. *Land Use Policy*, 82(January), 674-685. <https://doi.org/10.1016/j.landusepol.2018.11.058>
- 655 Duethmann, D. and Blöschl, G.2018. Why has catchment evaporation increased in the past 40 years? A data-based study in Austria. *Hydrology and Earth System Sciences*, 22, 5143-5158 <https://doi.org/10.5194/hess-22-5143-2018>.
- El Kateb, H., Zhang, H.F., Zhang, P.C., Mosandl, R. 2013. Soil erosion and surface runoff on different vegetation covers and slope gradients: A field experiment in Southern Shaanxi Province, 660 China. *CATENA* 105:1-10.
- Fan, X., Shi, C., Zhou, Y., Shao, W. 2012. Sediment rating curves in the Ningxia-Inner Mongolia reaches of the upper Yellow River and their implications. *Quaternary International*, 282, 152-162. <https://doi.org/10.1016/j.quaint.2012.04.044>.
- García-Ruiz, J. M. 2010. The effects of land uses on soil erosion in Spain?: A review. *CATENA*, 665 81(1), 1-11. <https://doi.org/10.1016/j.catena.2010.01.001>.
- Gascuel-Oudou, C., Arousseau, P., Doray, T., Squidant, H., Macary, F., Uny, D., Grimaldi, C. 2011. Incorporating landscape features to obtain an object-oriented landscape drainage network representing the connectivity of surface flow pathways over rural catchments. *Hydrological Processes* 25(23): 3625-3636.
- 670 Guzman, C. D., Tilahun, S. A., Zegeye, A. D., Steenhuis, T. S. 2013. Suspended sediment concentration-discharge relationships in the (sub-) humid Ethiopian highlands. *Hydrology and Earth System Sciences*, 17(3), 1067-1077. <https://doi.org/10.5194/hess-17-1067-2013>.
- Gyssels, G., Poesen, J., Bochet, E., Li, Y. 2005. Impact of plant roots on the resistance of soils to





- erosion by water: a review. *Prog. Phys. Geogr.* 29, 189-217.
- 675 Haslinger, K., Hofstätter, M., Kroisleitner, C., Schöner, W., Laaha, G., Holawe, F., & Blöschl, G. 2019. Disentangling Drivers of Meteorological Droughts in the European Greater Alpine Region During the Last Two Centuries. *Journal of Geophysical Research: Atmospheres*, 124(23), 12404–12425. <https://doi.org/10.1029/2018JD029527>
- Hou, J., Zhu, H., Fu, B., Lu, Y., Zhou, J. 2020. Functional traits explain seasonal variation effects of plant communities on soil erosion in semiarid grasslands in the Loess Plateau of China. *CATENA*, 194(June), 104743. <https://doi.org/10.1016/j.catena.2020.104743>.
- 680 Hu, B., Wang, H., Yang, Z., & Sun, X. 2011. Temporal and spatial variations of sediment rating curves in the Changjiang (Yangtze River) basin and their implications. *Quaternary International*, 230(1–2), 34–43. <https://doi.org/10.1016/j.quaint.2009.08.018>.
- 685 IUSS Working Group WRB. 2015. World Reference Base for Soil Resources 2014, update 2015 International soil classification system for naming soils and creating legends for soil maps. World Soil Resources Reports No. 106. FAO, Rome.
- Karvonen, T., Koivusalo, H., Jauhiainen, M. 1999. A hydrological model for predicting runoff from different land use areas. *J. Hydrol.* 217, 253-265.
- 690 Kelly, C.N., Mc Guire, K.J., Miniati, C.F., Vose, J.M. 2016. Streamflow response to increasing precipitation extremes altered by forest management. *Geophys. Res. Lett.* 43(8), 3727–3736. <https://doi.org/10.1002/2016GL068058>.
- Khaledian, H., Faghih, H., Amini, A. 2017. Classifications of runoff and sediment data to improve the rating curve method. *Journal of Agricultural Engineering*, 48(3), 147-153.
- 695 <https://doi.org/10.4081/jae.2017.641>.
- Kijowska - Strugata, M., Bucala - Hrabia, A., Demczuk, P. 2018. Long-term impact of land use changes on soil erosion in an agricultural catchment (in the Western Polish Carpathians). *Land Degrad. Dev.* 29:1871-1884.
- Korkanç, S. Y. 2018. Effects of the land use/cover on the surface runoff and soil loss in the 700 Niğde-Akkaya Dam Watershed, Turkey. *CATENA*, 163:233–243. <https://doi.org/10.1016/j.catena.2017.12.023>.
- Kottek, M., Grieser J., Beck, C., Rudolf, B., Rubel, F. 2006: World Map of the Köppen-Geiger climate classification updated. *Meteorol. Z.*, 15, 259-263. DOI: 10.1127/0941-2948/2006/0130.
- Kundzewicz, Z.W. (Ed.), 2012. Changes in Flood Risk in Europe. IAHS Special Publication 10,



- 705 516 pp.
- Li, S., Bing, Z., Jin, G. 2019. Spatially explicit mapping of soil conservation service in monetary units due to land use/cover change for the three gorges reservoir area, China. *Remote Sensing*, 11(4), 6-8. <https://doi.org/10.3390/rs11040468>.
- Li, Y., Li, J.J., Are, K. S., Huang, Z.G., Yu, H. Q., Zhang, Q.W. 2019. Livestock grazing significantly accelerates soil erosion more than climate change in Qinghai-Tibet Plateau: Evidenced from <sup>137</sup>Cs and <sup>210</sup>Pbex measurements. *Agriculture, Ecosystems & Environment* 285, doi:10.1016/j.agee.2019.106643.
- Lana-Renault, N., Latron, J., Karssenber, D., Serrano-Muela, P., Reguees, D., Bierkens, M. F. P. 2011. Differences in stream flow in relation to changes in land cover: A comparative study in two sub-Mediterranean mountain catchments. *Journal of Hydrology* 411(3-4):366-378.
- 715 Madarász, B., Jakab, G., Szalai, Z., Juhos, K., Kotroczó, Z., Tóth, A., Ladányi, M. 2021. Long-term effects of conservation tillage on soil erosion in Central Europe: A random forest-based approach. *Soil and Tillage Research*, 209. <https://doi.org/10.1016/j.still.2021.104959>.
- Madsen, H., Lawrence, D., Lang, M., Martinkova, M., Kjeldsen, T. R. 2014. Review of trend analysis and climate change projections of extreme precipitation and floods in Europe. *Journal of Hydrology*, 519, 3634 - 3650. <https://doi.org/10.1016/j.jhydrol.2014.11.003>
- Magliano, Patricio N., Whitworth-Hulse, Juan, I., Florio, Eva L., Aguirre, E.C., Blanco, L.J., 2019. Interception loss, throughfall and stemflow by *Larreadivaricata*: The role of rainfall characteristics and plant morphological attributes. *Ecological Research* 34(6):753-764.
- 725 Merriam, G. 1990. Ecological processes in the time and space farmland mosaics. In *Changing Landscapes: An Ecological Perspective*. 286 pp. Edited by S. Zonneveld and R.T.T. Forman, Springer-Verlag, New-York, pp. 121-126.
- Moghadam, B., Jabarifar, M., Bagheri, M., Shahbazi, E. 2015. Effects of land use change on soil splash erosion in the semi-arid region of Iran. *Geoderma* 241-242:210-220.
- 730 Moravcová, J., Koupilová, M., Pavlíček, T., Zemek, F., Kvítek, T., Pečenka, J. 2017. Analysis of land consolidation projects and their impact on land use change, landscape structure, and agricultural land resource protection: case studies of Pilsen-South and Pilsen-North (Czech Republic). *Landscape and Ecological Engineering*, 13(1), 1-13. <https://doi.org/10.1007/s11355-015-0286-y>.
- 735 Mullan, Donall. 2013. Soil erosion under the impacts of future climate change: Assessing the



- statistical significance of future changes and the potential on-site and off-site problems. *CATENA*. 109:234-246.
- Mullan, D., Matthews, T., Vandaele, K., Barr, I. D., Swindles, G. T., Meneely, J., Boardman, J., Murphy, C. 2019. Climate impacts on soil erosion and muddy flooding at 1.5 versus 2° C warming. *Land Degradation & Development* 30(1):94-108.
- 740
- Nampak, H., Pradhan, B., MojaddadiRizeei, H., Park, H. J. 2018. Assessment of land cover and land use change impact on soil loss in a tropical catchment by using multitemporal SPOT-5 satellite images and Revised Universal Soil Loss Equation model. *Land Degradation and Development*, 29(10), 3440-3455. <https://doi.org/10.1002/ldr.3112>.
- 745
- Nearing, M. A., Xie, Y., Liu, B., Ye, Y. 2017. Natural and anthropogenic rates of soil erosion. *International Soil and Water Conservation Research*, 5, 77-84. <https://doi.org/10.1016/j.iswcr.2017.04.001>.
- Nearing, M. A., Pruski, F. F., O'Neal, M. R. 2004. Expected climate change impacts on soil erosion rates: A review. *Journal of Soil and Water Conservation* 59 (1): 43-50.
- 750
- Nytch, C. J., Melendez-Ackerman, E. J., Perez, M., Ortiz-Zayas J.R.. 2019. Rainfall interception by six urban trees in San Juan, Puerto Rico. *URBAN ECOSYSTEMS*. 22(1): 103-115.
- Ozsahin, E., Duru, U., Eroglu, I. 2018. Land use and land cover changes (LULCC), a key to understand soil erosion intensities in the Maritsa Basin. *Water* 10(3). <https://doi.org/10.3390/w10030335>.
- 755
- Palazon, L., Navas, A. 2016. Land use sediment production response under different climatic conditions in an alpine–prealpine catchment. *CATENA* 137:244-255.
- Patin, J., Mouche, E., Ribolzi, O., Sengtahevhangoung, O., Latsachak, K.O., Soulileuth, B., Chaplot, V., Valentin, C. 2018. Effect of land use on interrill erosion in a montane catchment of Northern Laos: An analysis based on a pluri-annual runoff and soil loss database. *Journal of Hydrology* 563:480-494.
- 760
- Perović, V., Jakšić, D., Jaramaz, D., Koković, N., Čakmak, D., Mitrović, M., Pavlović, P. 2018. Spatio-temporal analysis of land use/land cover change and its effects on soil erosion (Case study in the Oplenac wine-producing area, Serbia). *Environmental Monitoring and Assessment*, 190 (11). <https://doi.org/10.1007/s10661-018-7025-4>.
- 765
- Phillips, R. W., Spence, C., & Pomeroy, J. W. 2011. Connectivity and runoff dynamics in



- heterogeneous basins. *Hydrological Processes* 25(19): 3061-3075.  
<https://doi.org/10.1002/hyp.8123>.
- 770 Prosdocimi, M., Cerdà, A., Tarolli, P. 2016. Soil water erosion on Mediterranean vineyards: A review. *CATENA*, 141, 1-21. <https://doi.org/10.1016/j.catena.2016.02.010>.
- Salesa, D., & Cerdà, A. 2020. Soilerosion on mountain trails as a consequence of recreational activities. A comprehensive review of the scientific literature. *Journal of Environmental Management*, 271(June). <https://doi.org/10.1016/j.jenvman.2020.110990>.
- 775 Santos, J.C.N., de Andrade, E.M., Medeiros, P.H.A., Guerreiro, M.J.S., Palacio, H.A.D. 2017. Effect of Rainfall Characteristics on Runoff and Water Erosion for Different Land Uses in a Tropical Semiarid Region. *Water Resources Management* 31(1):173-185.
- Scholz, G., Quinton, J.N., Strauss, P., 2008. Soil erosion from sugar beet in Central Europe in response to climate change induced seasonal precipitation variations. *CATENA* 72, 91–105. <https://doi.org/10.1016/j.catena.2007.04.005>.
- 780 Sharma, A., Tiwari, K. N., Bhadoria, P. B. S. 2011. Effect of land use land cover change on soil erosion potential in an agricultural watershed. *Environmental Monitoring and Assessment*, 173(1-4), 789-801. <https://doi.org/10.1007/s10661-010-1423-6>.
- Sheridan, G. J., Lane, P. N. J., Sherwin, C. B., Noske, P. J. 2011. Post-fire changes in sediment rating curves in a wet Eucalyptus forest in SE Australia. *Journal of Hydrology*, 409(1-2), 183-195. <https://doi.org/10.1016/j.jhydrol.2011.08.016>.
- 785 Silasari, R., Parajka, J., Ressler, C., Strauss, P., and Blöschl, G. 2017. Potential of time-lapse photography for identifying saturation area dynamics on agricultural hillslopes. *Hydrological Processes*, 31, 3610–3627, doi: 10.1002/hyp.11272.
- Silva, R.M., Santos, C.A.G., Santos, J.Y.G. 2017. Evaluation and modeling of runoff and sediment yield for different land covers under simulated rain in a semiarid region of Brazil. *Int. J. Sediment Res.* <http://dx.doi.org/10.1016/j.ijsrc.2017.04.005i>.
- 790 Sun, D., Yang, H., Guan, D., Yang, M., Wu, J.B., Yuan, F.H., Jin, C.J., Wang, A.Z., Zhang, Y.S. 2018. The effects of land use change on soil infiltration capacity in China: A meta-analysis. *Science of the Total Environment* 626: 1394-1401.
- 795 Sun, P.C., Wu, Y.P., Wei, X.H., Sivakumar, B., Qiu, L.J., Mu, X.M., Chen, J., Gao, J.E. 2020. Quantifying the contributions of climate variation, land use change, and engineering measures for dramatic reduction in streamflow and sediment in a typical loess watershed, China. *Ecological*



- engineering. 142. <https://doi.org/10.1016/j.ecoleng.2019.105611>.
- Sun, W.Y., Shao, Q.Q., Liu, J.Y. 2013. Soil erosion and its response to the changes of precipitation  
800 and vegetation cover on the Loess Plateau. *JOURNAL OF GEOGRAPHICAL SCIENCES*  
23(6):1091-1106.
- Smakhtin, V.U. 2001. Low flow hydrology: a review. *Journal of Hydrology*, 240 (3-4), 147-186.
- Syvitski, J.P., Morehead, M.D., Bahr, D.B., Mulder, T. 2000. Estimating fluvial sediment transport:  
the rating parameters. *Water Resour. Res.* 36 (9), 2747-2760.
- 805 Syvitski, J.P.M., Alcott, J.M. 1995. RIVER3: simulation of water and sediment river discharge  
from climate and drainage basin variables. *Comput.Geosci.*21, 89-151.
- Takken, I., Beuselinck, L., Nachtergaele, J., Govers, G., Poesen, J., Degraer, G. 1999. Spatial  
evaluation of a physically-based distributed erosion model (LISEM). *Catena*. 37: 431-447.
- Tang, C., Liu, Y., Li, Z., Guo, L., Xu, A., Zhao, J. 2021. Effectiveness of vegetation cover pattern  
810 on regulating soil erosion and runoff generation in red soil environment, southern China.  
*Ecological Indicators*, 129, 107956. <https://doi.org/10.1016/j.ecolind.2021.107956>.
- Thomas, R. B. 1988. Monitoring baseline suspended sediment in forested basins: the effects of  
sampling on suspended sediment rating curves. *Hydrological Sciences Journal*. 33,5- 10.
- USDA-Staff. 2019. Rainfall intensity summarisation tool (RIST)in.  
815 <https://www.ars.usda.gov/southeast-area/oxford-ms/national-sedimentation-laboratory/watershed-physical-processes-research/research/rist> (Accessed in January, 2020)
- Van Oost, K., Govers, G., Desmet, P. 2000. Evaluating the effects of changes in landscape  
structure on soil erosion by water and tillage. *Landscape Ecology*, 15(6), 577-589.  
<https://doi.org/10.1023/A:1008198215674>.
- 820 Van Rompaey, A.J.J., Verstraeten, G., van Oost, K., Govers, G., Poesen, J. 2002. Modelling mean  
annual sediment yield using a distributed approach. *Earth Surface Processes and Landforms*  
26:1221-1236.
- Vanmaercke, M., Zenebe, A., Poesen, J., Nyssen, J., Vertstraeten, G., and Deckers, J. 2010.  
Sediment dynamics and the role of flash floods in sediment export from medium-sized catchments:  
825 a case study from the semi-arid tropical highlands in northern Ethiopia, *J. Soil. Sediment.* 10:  
611-627.
- Vaughan, A. A., Belmont, P., Hawkins, C. P., Wilcock, P. 2017. Near-Channel Versus Watershed  
Controls on Sediment Rating Curves. *Journal of Geophysical Research: Earth Surface*, 122(10),



- 1901-1923. <https://doi.org/10.1002/2016JF004180>.
- 830 Wang, L.J., Zhang, G.H., Wang, X., Li, X.Y. 2019. Hydraulics of overland flow influenced by litter incorporation under extreme rainfall. *Hydrological Processes* 33(5):737-747.
- Wang, J., Shi, X., Li, Z., Zhang, Y., Liu, Y., Peng, Y. 2021. Responses of runoff and soil erosion to planting pattern, row direction, and straw mulching on sloped farmland in the corn belt of northeast China. *Agricultural Water Management*, 253(December 2020), 106935.
- 835 <https://doi.org/10.1016/j.agwat.2021.106935>
- Wang, S.P., McVicar, Tim R., Zhang, Z.Q., Brunner, T., Strauss, P. 2020. Globally partitioning the simultaneous impacts of climate-induced and human-induced changes on catchment streamflow: A review and meta-analysis. *Journal of Hydrology*. <https://doi.org/10.1016/j.jhydrol.2020.125387>.
- Warrick, J.A., Rubin, D. M., 2007. Suspended-sediment rating curve response to suburbanization and wildfire, Santa Ana River, California. *Journal of Geophysical Research*. 112, F02018, doi:10.1029/2006JF000662.
- Wei, W., Chen, L., Fu, B., Huang, Z., Wu, D., Gui, L. 2007. The effect of land uses and rainfall regimes on runoff and soil erosion in the semi-arid loess hilly area, China. *J. Hydrol.* 335, 247-258.
- 845 Yao, J.J., Cheng, J.H., Zhou, Z.D., Sun, L., Zhang, H.J. 2018. Effects of herbaceous vegetation coverage and rainfall intensity on splash characteristics in northern China. *Catena* 167:411-421.
- Zhang, G.H., Liu, G.B., Wang, G.L., Wang, Y.X. 2011. Effects of vegetation cover and rainfall intensity on sediment-associated nitrogen and phosphorus losses and particle size composition on the Loess Plateau. *Journal of Soil and Water Conservation* 66(3):192-200
- Zhang, X.C., Nearing, M.A. 2005. Impact of climate change on soil erosion, runoff, and wheat 850 productivity in central Oklahoma. *Catena* 61:185-195.
- Zhang, X.A., She, D., L., Hou, M., T., Wang, G.B., Liu, Y. 2021. Understanding the influencing factors (precipitation variation, land use changes and check dams) and mechanisms controlling changes in the sediment load of a typical Loess watershed, China. *Ecological Engineering* 163. <https://doi.org/10.1016/j.ecoleng.2021.106198>.
- 855 Zhang, Y., Xu, C., & Xia, M. 2021. Can land consolidation reduce the soil erosion of agricultural land in hilly areas? Evidence from Lishui district, Nanjing city. *Land*, 10(5). <https://doi.org/10.3390/land10050502>.